NOVEL LEAD FREE BRONZE BEARING MATERIALS PRODUCED BY POWDER METALLURGY PROCESSING

Greg Vetterick[1,2], Iver Anderson[1,2], Matt Besser[2]

[1]Iowa State University; Ames, Iowa 50012, USA
US Department of Energy Ames Laboratory; Ames, Iowa, 50012

ABSTRACT

Leaded bronze alloys such as Cu-10Sn-10Pb (wt.%) are utilized effectively in tribological systems that are prone to lubrication starvation. These Cu-based leaded alloys typically exploit the insolubility of lead in copper to create soft phase pockets in the microstructure on solidification of a chill casting or consolidation of gas atomized powder. Properly distributed throughout the bearing, free lead provides a low shear solid lubricant for sliding interfaces. However, the toxicity of lead necessitates the development of alternatives for the soft lead phase. The current work explores replicating the desirable microstructure of leaded bronze by utilizing powder metallurgy processes. Impregnation of a bronze matrix microstructure with lead-free soft alloys shows considerable promise as a bearing alloy production method. Microstructural analysis and tribological evaluation of the resulting composite bearings helped verify adequate performance as a lead-free bearing system. This work is supported by Sauer Danfoss, Inc as Work for Others through US Department of Energy Ames Laboratory Contract No. DE-AC02-07CH11358. Protected under U.S. Provisional Patent No. 61/337,672.

INTRODUCTION

Bearings play a vital role in any engineered system with moving parts. In conjunction with lubricants, bearings increase the lifetime and efficiency of the machine. Material selection for the moving components in tribological systems is driven by the application, often requiring a balance of properties to ensure suitable performance. Such a case is exemplified during the breakdown of the lubricating film in hydrodynamically lubricated systems. When lubrication is provided by the relative movement of the interfaces, the possibility exists for lubricant starvation resulting in direct contact of the two surfaces. To prevent subsequent damage to the component and bearing surfaces, a dual-phase material is often employed.

Leaded bronze bearing alloys are a prime example of a material used in hydrodynamically lubricated applications. The properties of the two constituents, lead and bronze, are balanced as a composite material that helps maintain the lubricating film and prevents damage in the event of film breakdown. The microstructure of the leaded bronze bearing makes use of the insolubility of lead in copper to create free globules of lead in a copper-tin matrix when produced by casting [1]. The soft lead phase deforms easily and is smeared across the surface to form a low shear solid lubricant at high sliding velocities, thereby preventing seizure during lubrication starvation [2]. In addition, the lead pockets minimize the effect of abrasive wear particles during normal operation. The tough support structure of α (FCC) phase bronze provides the strength and fatigue characteristics of the bearing surface [1].

Leaded bronze bearings are effective; however, the plight of lead-based bearing alloys is analogous to that of lead-bearing solders that are facing increasing pressure for replacement. The primary source of this movement is European Union Directive 2002/95/EC entitled the Restriction of Hazardous Substances Directive (RoHS). RoHS requires substitutions for various heavy metals in new electrical and electronic equipment. The language of the directive originally included the entire gamut of engineering applications, including bearing alloys. Exemptions were ultimately made for many applications including “lead in lead-bronze bearing shells and bushes” [3]. These concessions freed up the use of leaded bronze bearing alloys until suitable replacements could be found. Concerns thus exist about the use of lead in bearing alloys, and alternative bronze materials have been produced that mimic the success of the leaded bronze’s multicomponent structure. A subset of these materials is being developed to possess a microstructure similar to a common cast leaded bronze alloy consisting of 10% tin, 10% lead and the remainder copper (wt. %).

The Cu-10Sn-10Pb alloy is commonly used in axial piston hydraulic pumps as a sliding pair with a proprietary copper-infused steel surface. The interface is hydrodynamically lubricated by ISO 46 grade hydraulic fluid [6]. Previous investigation into the nature of wear in hydraulic pumps suggested that the pressure differential in an axial piston hydraulic pump or slight mechanical imbalances can lead to increased normal force on the bearing surface. This force results in direct contact and a phenomenon colloquially known as “heat checking” that represents the most severe wear conditions in the pump [5,6]. As with all hydrodynamically lubricated applications, the bearing material must minimize the damage caused by unexpected solid contact due to misalignment, high load or slow speed at the sliding interface. It is in these regions that lead- and tin-based alloys work optimally. In addition to their ability to deform to the mating surface in this scenario, these soft alloys can flow or even melt to protect the surfaces from damage [7]. This is the direct intent of the Cu-10Sn-10Pb alloys which provide pockets of soft lead for just such a purpose.

As a replacement for the currently employed Cu-10Sn-10Pb alloy, Federal Mogul designed a Cu-10Sn-3Bi (wt.%) bronze meant to utilize the insolubility of bismuth to create a soft second phase similar to the leaded bronze alloys [4]. The composition demonstrated good wear characteristics in automotive applications, including increased fatigue and corrosion resistance. However, testing in axial piston hydraulic pumps showed that the Cu-10Sn-3Bi material was unsuitable as a bearing material for that application [5]. Bearing loads of up to 2.54 MPa (368 psi), a PV factor of 3.72 x 107 N/m s (212,000 lb/in s) and lubricating oil temperatures exceeding 130°C (266°F) promote the formation of a liquid bismuth-tin alloy [5,6]. The presence of liquid bismuth causes liquid metal embrittlement [5]. The Cu-10Sn-3Bi example illustrates that the limiting wear characteristics in this case are determined by the soft phase.

Selection of a Pb-free alternative is therefore critical for more demanding applications. Fortunately, while the attempt to use bismuth to reproduce the composite type of microstructure including insoluble phases is commendable, it is not required given the technologies available in powder metallurgy. In fact, existing methods in powder metallurgy and bearing metal alloying provide a basis from which to develop lead-free, bronze-based metal/metal composite bearings.

ALLOY CONCEPT

In addition to multi-component leaded bronze alloys, hydrodynamically lubricated applications often employ multilayered journal bearings. These bearings, at their simplest, consist of a steel backing material for strength, a copper-based interlayer for fatigue resistance and a Babbit metal surface layer to reduce the effect of abrasive particles and metal-to-metal contact. The similarities between the structure of the journal bearings and leaded bronze alloys provide inspiration for a new material. In journal bearings, tin-based Babbit alloys have been used for decades nearly interchangeably with lead-based bearing materials. Although their cost is somewhat higher, tin-based Babbits are generally considered superior to the lead-based alternatives. Additions of copper and antimony result in fine dispersoid intermetallic phases that increase the fatigue strength of the alloy below a temperature of 130˚C (266°F) while having no detrimental effect on the bearing properties [1]. Copper is added to introduce a hard primary Cu_6Sn_5 intermetallic, and the antimony content of the alloys is manipulated to add a secondary SbSn intermetallic at antimony levels over 7.5 wt.% [1].

The relative success of tin-based alloys over their lead-based counterparts provided sufficient motivation to create a new material with a microstructure similar to that of the leaded bronzes; that is, free pockets of the soft metal in a bronze matrix. The selection of a tin alloy as a soft phase in a bronze substrate does present challenges because its solubility provides the opportunity for the Cu_6Sn_5 copper-tin intermetallic to form where the tin is in contact with bronze, as commonly seen in solder joints. While dispersed precipitates of the intermetallic phases improve mechanical properties, having a continuous boundary of the hard, brittle phase may prove to be a detriment to wear properties. To avoid breakup of the hard phase, and thus possible poor wear performance of the valve plate, the amount of Cu_6Sn_5 at the interface should be controlled. Initial reduction of the Cu_6Sn_5 intermetallic can be achieved by limiting time at temperature during reflow. This, in turn, requires the development of a relatively precise processing technique.

Alloying additions can also suppress Cu_6Sn_5 formation, many of which are the subject of intense scrutiny in the lead-free solder arena. One of the additions under consideration for such properties is manganese. When alloyed at 1-9 wt.%, a relatively low melting (230.85°C, 447.53°F) eutectic is formed which is substantially higher than the tin-bismuth eutectic present in the Cu-10Sn-3Bi alloy. The addition of manganese would create a solid solution of tin and manganese with a slightly higher hardness than pure tin and contain hard, needle-like $MnSn_2$ intermetallics. It is expected that this intermetallic phase would provide some structural stability above the 230.85°C (447.53°F) solidus temperature of the alloy, above which a mushy, partially melted metal would be present. The result of proper processing techniques and alloying additions should be a microstructure as illustrated below. The aim is to acquire a distribution of the soft phase in the pores between sintered bronze powder particles, similar to the leaded bronze and the bismuth-bronze alloy.

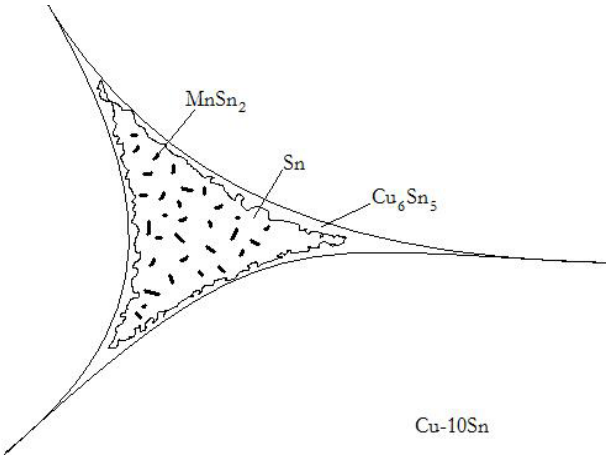

Figure 1. Optimum soft phase microstructure for the proposed composite bearing material.

The required microstructure would be virtually impossible to produce using admixed powder and liquid phase sintering. The relatively high temperatures and extended times required to sinter bronze powder would result in dissolution of the tin into the Cu-10Sn matrix. In fact this is a widely employed method of producing fully dense bronze compacts. However, powder metallurgy offers alternate solutions to this problem. Infiltration is routinely utilized to fill interconnected porosity or surface porosity in PM components. This is done for a number of reasons, not the least of which is wear properties. There are many examples of this in various industries. For instance, refractory metals (W and Mo) are infused with highly conductive metals (Ag, Cu) for heavy duty electrical contacts; iron and steel are infiltrated with copper for machinability; and iron and copper are infused with lead as low friction bearing materials [9].

MATERIAL PREPARATION

Infiltration requires first sintering a compact of the higher melting metal alloy to produce interconnected porosity to allow full penetration of the lower melting metal by capillary forces. Infiltration of the second, lower melting metal can be done by placing the infiltrant alloy in contact with the sintered compact in various forms including powder, a slug or already molten liquid. For the current study, a powder form of the alloy was chosen to provide even coverage of the bronze compact surface. The target tin alloy (1-9 wt.% Mn) was close-nozzle gas jet atomized in an argon atmosphere. The target particle size was less than 20µm, such that a carrier could be used to deposit the powder evenly on the surface of the bronze compacts. Atomization by HJE Company, Inc. produced a tin manganese powder with a composition of 1.37% Mn (verified by inductively coupled plasma (ICP) atomic emission spectrometry). The Sn-1.37Mn powder was sieved using -325 mesh to obtain a distribution with a d10 of 3.23µm, d50 of 7.81µm and d90 of 15.48µm.

The sintered bronze compacts for subsequent infusion experiments were created using 2.750±0.001g (0.97 oz) of commercially available 90Cu-10Sn bronze powder sieved to between 45µm and 75µm. The powder was pressed in a 12.7mm (0.5in) diameter cylindrical single acting die comprised of a carbide sleeve press fit in tool steel. Compaction pressures from 100-700MPa (14.5-101.5 ksi) were attempted to create compacts approximately 3.2mm (1/8in) thick with varying green densities. It was found that pressures less than 350MPa (50.8 ksi) did not provide sufficient green strength for handling of the compacts. Samples compressed between 350MPa and 700 MPa (50.8 ksi and 101.5 ksi), the upper limit of the die, were thus used to determine proper sintering parameters for optimum porosity.

Samples pressed at 350MPa and 700MPa were vacuum sintered at 10^{-5} torr for two hours at 400˚C, 500˚C, 600˚C, and 780˚C (752˚F, 932˚F, 1112˚F, 1436˚F), the latter chosen based on Nenakhov's work [10]). It was found that temperatures below 600˚C (932˚F) were not sufficient to create enough necking to provide adequate strength of the final bronze compact. At 600˚C (932˚F), necking increased to 30-50% of the particle diameter, ensuring adequate strength of the sintered bearing. Samples pressed at 550MPa (79.8 ksi) and sintered at 780˚C (1436˚F) were chosen for initial experiments to determine whether the material could be made with a strength approaching that of conventional cast bronze.

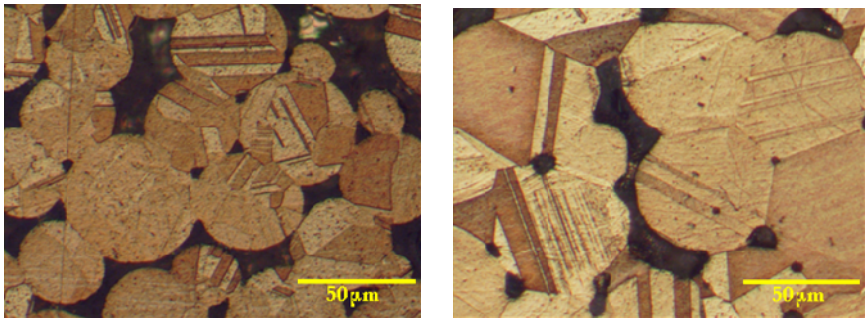

(a) (b)

Figure 2. Necking in bronze compacted at 550MPa and sintered at (a) 600˚C and (b) 780˚C

For initial study, the 12.7mm (½ in) diameter presintered, 550MPa/780˚C/2hr (79.8 ksi, 1436˚F, 2hr), bronze compacts were coated with a slurry of tin-manganese powder in methanol. The mixture was poured onto the sample surface until it was completely coated and allowed to dry, resulting in a coating of powder approximately 1.5mm (1/16 in) thick. The coated compacts were placed under a vacuum of 10^{-5} torr for 12 hours, after which they were sealed in 15mm (0.59 in) quartz tubes under 1/3 atm gettered argon. For the heat treatment, the quartz tubes were placed individually into a furnace preheated to 450˚C (842˚F) and observed until coalescence of the tin alloy on the surface was discerned. When this condition was reached, the samples were removed from the furnace and the quartz tubes broken to allow a water quench of the sample. As shown in Figure 3, initial samples displayed only partial coalescence of tin-manganese powder on the surface even after reaching 425˚C (797˚F).

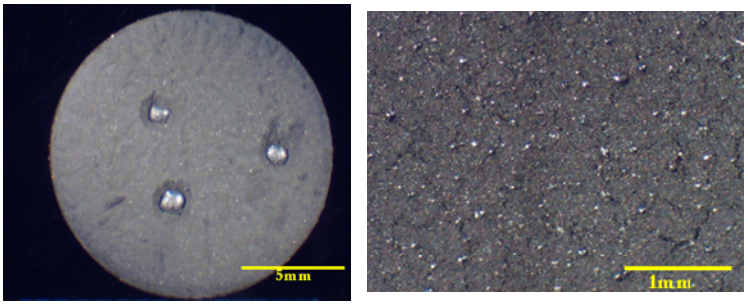

Figure 3. Partial coalescence of Sn-1.37Mn on bronze compacts.

A cross-section of the compact (Figure 4) shows that the Sn-1.37Mn powder particles have partially coalesced, and only a small about of liquid made it to the surface for impregnation. A small pocket can be observed subsurface; however, using the energy dispersive spectroscopy (EDS) capability of the scanning electron microscope (SEM), it was determined that the pocket consists of primarily Cu_6Sn_5 intermetallic separated from the bronze by a layer of Cu_3Sn. This morphology is not desired for a bearing alloy requiring a soft second phase.

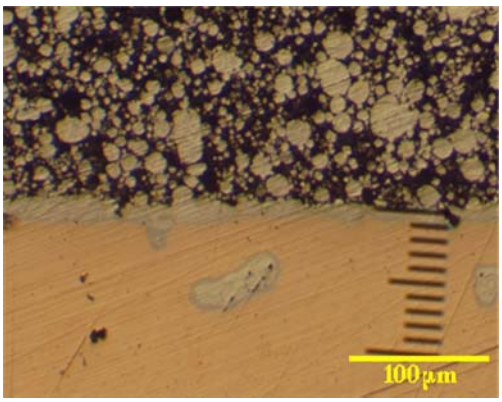

Figure 4. A polished cross-section of the sample shown in Figure 3.

The excessive growth of the intermetallic phases indicate that the temperature of infiltration must be lowered. In addition, effective infiltration requires full contact with, and wetting of, the presintered compact. Issues during the production of the Sn-1.37Mn alloy had previously suggested that atmospheric contamination, specifically with nitrogen, played a significant role in the ability of the material to melt. To test this theory in the context of infusion, the experiment was repeated with sub-25µm (< 0.98mil) pure tin powder. As Figure 5 illustrates, there is a significant difference between the melting coalescing capabilities of Sn-1.37Mn and pure Sn powders in a partial vacuum.

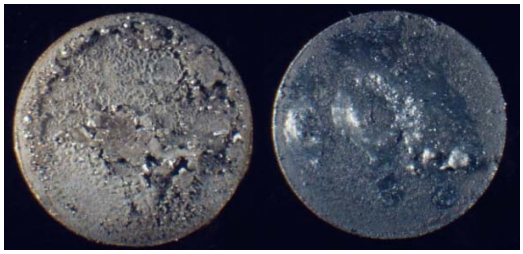

(a) (b)

Figure 5. (a) Sn-1.37Mn and (b) Sn powders after equivalent heat treatment.

Differential scanning calorimetry (DSC) was used to determine whether the Sn-1.37Mn alloy was simply not reaching a liquid state during the procedure or whether the problem lay in coalescence. For the DSC runs, 14mg of powder was placed in pure copper pans and heated from 50˚C at 20˚C/min to 450˚C then cooled at 60˚C/min to 50˚C (from 122˚F at 68˚F/min to 842˚F, then cooled at 140˚F/min to 122˚F). The results showed that the onset of melting for Sn-1.37Mn (230.8˚C, 447.4˚F) was only 0.2 degrees higher than that of pure Sn (230.6˚C, 447.0˚F). These temperatures compare reasonably well with those predicted by their respective phase diagrams; that is, 230.85 ˚C (447.53˚F) for Sn-1.37Mn and 231.95˚C (449.51˚F) for pure Sn. Observation of the powders after DSC runs showed similar results to those shown in Figures 4 & 5. The Sn-1.37Mn alloy coalesced significantly less than the pure Sn, suggesting that an oxide or nitride shell on the Sn-1.37Mn powder prevents coalescence required for proper infiltration of the bronze compact.

Given proper control of atmospheric conditions within the quartz tubes, infiltration of the porous bronze is possible. In the sample shown below in Figure 6, a presintered, 550MPa/780˚C/2hr (79.8 ksi, 1436˚F, 2hr) bronze compact was successfully infiltrated to adequate depth (approximately 600µm) required for steel-backed sintered bronze bearing materials.

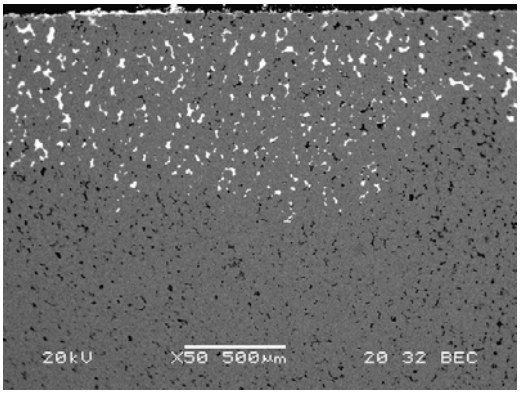

Figure 6. Backscattered electron image of Sn-1.37Mn (shown in white) penetration depth.

The filled porosity of the sample shown in Figure 6 is depicted in a larger view in Figure 7. The microstructure closely mimics that foreshadowed in Figure 1. The microstructure consists of a pocket of pure tin rimmed with Cu_6Sn_5 intermetallic. EDS was used to confirm the identity of the phase at the pore boundary. Backscattered electron imaging in the scanning electron microscope shows embedded Cu_6Sn_5 in the center of the pore. Recalling the properties of many tin Babbit materials, this intermetallic phase is known to improve the fatigue properties of the alloy and is not seen as a detriment to the alloy's structure.

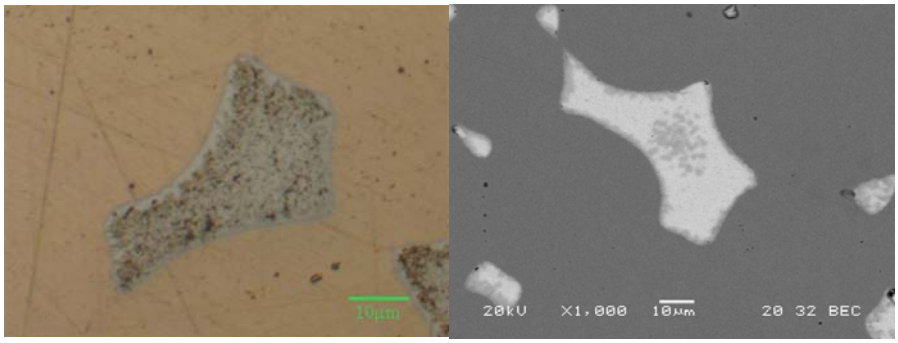

(a) (b)

Figure 7. Optical (a) and backscattered (b) images of the infiltrated pores.

Although promising, the overview image in Figure 6 shows that the distribution of tin is not even in the presintered 550MPa/780˚C/2hr (79.8 ksi, 1436˚F, 2hr) compact. There are pores visible which were not filled with Sn-1.37Mn upon infiltration, indicating a lack of interconnected porosity. In addition, the depth of penetration is not consistent across the entire surface of the 12.7mm (1/2 in) presintered compact. While the remaining porosity is not necessarily detrimental to the performance of the alloy in lubricated environments, the objective of the current work is to create an even distribution of solid lubricant in the bronze to a depth of at least 0.5mm (0.02 in), the minimum desired thickness of a steel-backed bearing.

Closer examination of the microstructure in the bronze compacts (Figure 8) after compaction at 550MPa (79.8 ksi) and two hours sintering at 780˚C (1436˚F) shows that porosity may not be fully interconnected in some regions of the compact. Porosity of these samples was determined to be approximately 10 volume percent by optical microscopy. To alleviate this problem, subsequent samples were pressed at a lower, 350MPa (50.8 ksi) compaction pressure and sintered at 650˚C (1202˚F) for two hours. This heat treatment allowed for the maximum porosity (19 vol%) while still retaining significant strength.

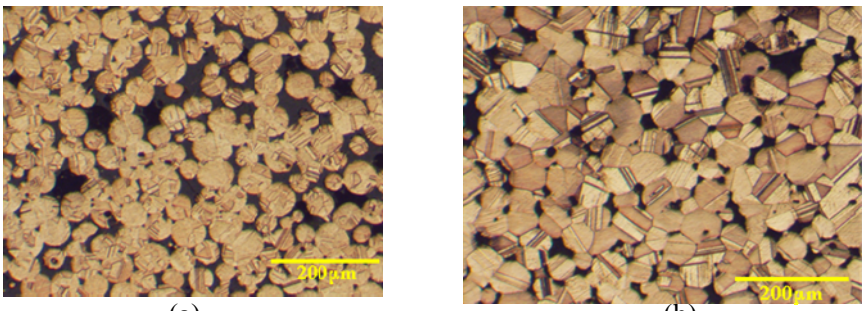

(a) (b)

Figure 8. Bronze compacted and sintered at (a) 350MPa, 650˚C, 2hrs & (b) 550MPa, 780˚C, hrs.

Interconnected porosity is only one part of the requirements for infiltration. Improvements in available material and wetting are required to ensure full impregnation of the bronze compact. To eliminate the poor Sn-1.37Mn powder coalescence and provide a clean bronze surface for proper wetting, the decision was made to utilize a flux. Using a flux provides greater control over the final microstructure and prevention of intermetallic growth by decreasing the time required for full coalescence of the bronze compact. Providing a clean bronze surface increases the wetting of the tin on the bronze, thus increasing the capillary force available to draw the alloy into the interconnected porosity.

Two thermally activated chloride-based fluxes, E 127 and E 130, were acquired from Johnson Manufacturing Company. Pastes were created using each flux in combinations with the pure tin and Sn-1.37Mn powders in the weight ratios suggested by the manufacturer. Drops of the pastes were then placed on presintered, 350MPa/650˚C/2 hr (50.8 ksi/1202˚F/2hr) compacts of the 90Cu-10Sn bronze. These samples were placed on a hotplate preheated to 250°C (482˚F) in an argon atmosphere and observed until coalescence for greater processing control. Upon coalescence the samples were removed and placed on a copper chill block for a mass quench. The resultant sample is shown below in Figure 9. Although a small amount of Sn-1.37Mn was placed on the sample, the metal infiltrated to a nearly uniform depth of 2mm (0.08 in).

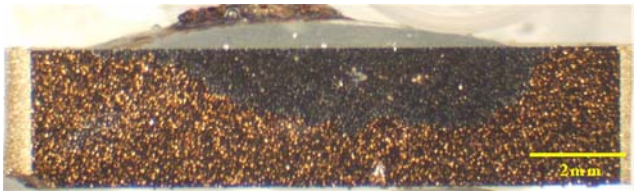

Figure 9. Infiltration of Sn-1.37Mn alloy into a 90-10Sn compact using E127 flux.

In addition to effective infiltration, the soft tin metal is evenly distributed in the compact and possesses the target morphology consisting primarily of the soft phase with minimal intermetallic rim as shown in the images in Figure 10.

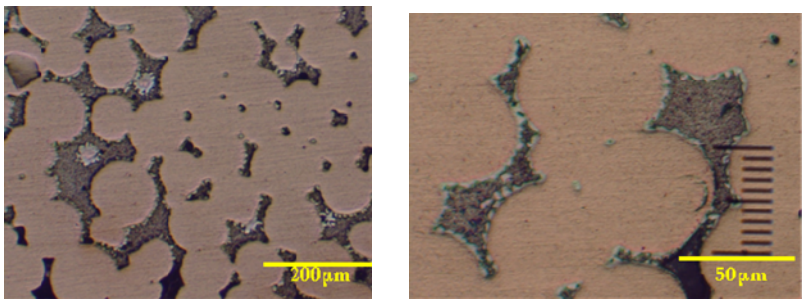

Figure 10. Polished surface showing pockets of Sn-1.37Mn in Cu-10Sn bronze with Cu_6Sn_5 rims.

When the morphology of the original Cu-10Sn-10Pb alloy, the Federal Mogul Cu-10Sn-3Bi and the newly created Cu-10Sn/Sn-1.37Mn composite material are compared using secondary electron imaging in the scanning electron microscope, the similarities are clear. The size and distribution of the soft phase pockets in the new composite are very similar to that of the two previous alloys and are depicted in Figure 11.

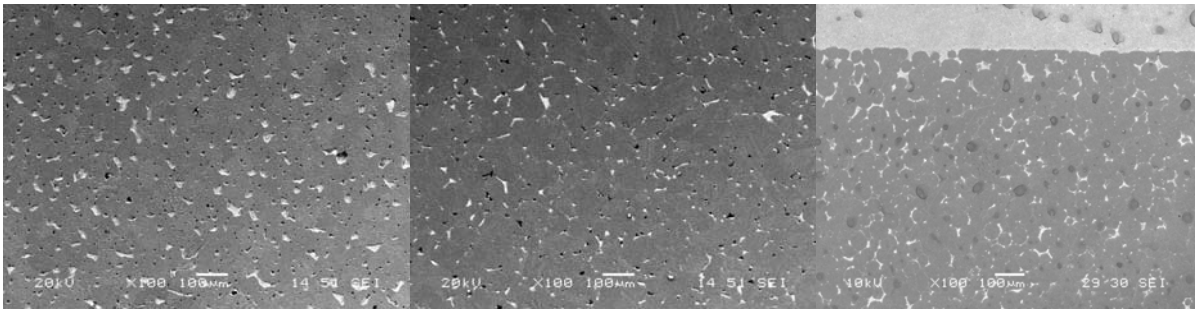

(a) (b) (c)

Figure 11. Distribution of the soft phases in (a)Cu-10Sn-10Pb (b) Cu-10Sn-3Bi and (c) Sn-1.37Mn infused Cu-10Sn.

VALIDATION

The Cu-10Sn/Sn-1.37Mn and Cu-10Sn/Sn metal-metal composite materials show promise as replacements for Cu-10Sn-10Pb leaded bronze in terms of microstructure. To evaluate their performance as bearing materials, characterization of the material in terms of mechanical, life and wear properties was required. In order to be effective, the engineered microstructure of the tin-infiltrated bronze must only contain a small amount of intermetallic phase along the edges of the pockets. The intermetallics possess properties that may be beneficial in small amounts, but mechanical issues brought on by thick layers of the brittle copper-tin intermetallics must be mitigated. Unfortunately, operating oil temperatures in lubricated systems such as axial piston hydraulic pumps are high enough to promote the growth of Cu_6Sn_5 and Cu_3Sn intermetallics at the copper-tin interface. Axial piston hydraulic pumps are capable of running up to 10,000 hours at temperatures reaching as high 130°C (266˚F) resulting from frictional and other fluid losses throughout the hydraulic system Therefore aging tests were critical to determine the lifetime of the soft phase and thus the effective lifetime of the bearing.

Samples prepared in the maximum porosity condition (350MPa/ 650˚C/2 hr or 50.8 ksi/1202˚F/2hr) were thermally aged zero hours, 100 hours, and 750 hours at 130±1°C (266˚F) to replicate the conditions present in axial piston hydraulic pumps. The results of the aging tests are shown below in Table I.

Table I: Intermetallic Layer Thickness (in micrometers) at Various Aging Times

		Aging Time		
		0 hrs	100 hrs	750 hrs
Sn	Cu_6Sn_5	1	1.6	2.5
	Cu_3Sn	0	1.4	2.7
	Total	1	3	5.2
Sn-1.37Mn	Cu_6Sn_5	0.87	1.25	3.2
	Cu_3Sn	0	0.35	1.7
	Total	0.87	2.6	4.9

The porous bronze compacts infiltrated with both Sn-1.37Mn and pure Sn had similar initial intermetallic layer thicknesses if processed properly, i.e. kept near the 250˚ C (482˚F) reflow temperature for the shortest possible time. Upon aging, the samples infiltrated with Sn-1.37Mn possess a slightly lower total intermetallic thickness than their Sn-infiltrated counterparts. The more substantial difference comes in the suppression of the Cu_3Sn layer through the aging process.

In addition to producing elevated temperatures during operation, the action in the pump induces substantial stresses in the valve plate. It is important then to evaluate the strength of the new bearing material. The porosity and strength would eventually need to be balanced for the optimum bearing material design. Strength tests were performed to measure transverse rupture strength (TRS) according to ASTM standards B528-05 and B925-03. TRS bar specimens were compacted and sintered at 350MPa (50.8 ksi) and 650°C (1202˚F) then infiltrated with pure tin. Of the samples prepared in this manner, one set was aged 100 hours before testing, and the other set was tested as-infiltrated. An Instron model 55R1125 test frame was used to measure transverse rupture strength, incorporating a fixture designed according to ASTM specifications. The Instron was set to deflect the sample at a rate of 0.05 in/min. The force required was recorded as a function of deflection distance and used to calculate the transverse rupture strength.

For the ease of initial production, samples produced throughout this study were made from bronze compacts pressed at 350MPa(50.8 ksi) then sintered at 650˚C (1202˚F) for 2 hours. Keeping in mind that the 350MPa/650˚C/2hr (50.8 ksi/1202˚F/2hr) compact production parameters were specifically chosen to maximize the ease of infiltration while sacrificing strength, the results from the TRS tests can be compared to the existing Cu-10Sn-Pb and experimental Cu-10Sn-3Bi strength data provided by Federal Mogul [4]. This comparison is shown in Figure 12.

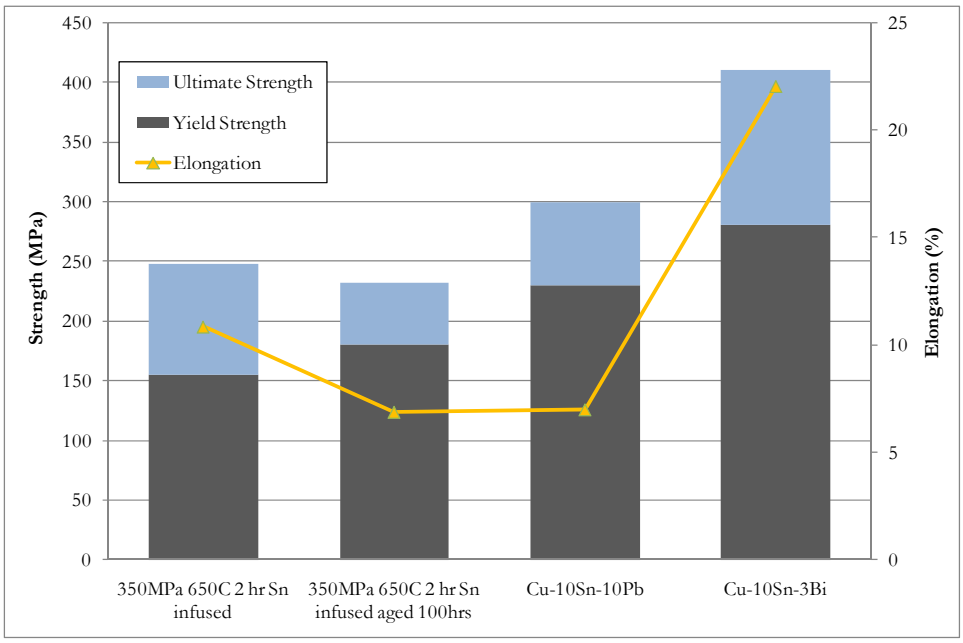

Figure 12. Comparison of mechanical properties to previous alloys.

The alloy developed for this study, the tin-infiltrated bronze, displayed mechanical properties that approached that of the leaded and bismuth bronze alloys previously developed. The results of tests relating compaction pressure and sintering time and temperature to strength show that increases in either parameter can and will increase the yield strength, ultimate strength, and elongation of the bronze compacts. In addition, samples have already been successfully infiltrated using a compaction pressure of 550MPa (79.8 ksi) and sintering at 780˚C (1436˚F) for 2 hours. Using these increased variables to create the sintered compact would result in mechanical properties on par with or exceeding those of the previous alloys.

The most important qualification for a bearing material is its wear performance. In the current study, the objective was to replace the current Cu-10Sn-10Pb bronze and outperform the experimental Cu-10Sn-3Bi material that provide a low friction, wear resistant bearing materials in axial piston hydraulic pumps. Therefore, a wear test was developed to directly compare the newly developed Cu-10Sn/Sn-1.37Mn and Cu-10Sn/Sn materials with the Cu-10Sn-10Pb and Cu-10Sn-3Bi materials. The test, based on the standard pin-on-disk test method as defined by ASTM G99-05, was designed to mimic the conditions in the hydraulic pump.

A Falex ISC250PC tribometer was modified to attempt to provide the lubrication, load, and sliding speeds present in axial piston hydraulic pumps. Lubrication in axial piston hydraulic pumps is provided by the hydraulic fluid that is heated by friction and system losses. For the purposes of this study, ISO-46 grade Shell Tellus Plus hydraulic fluid was heated to a temperature between 80°C and 130°C (176°F-266°F) and permitted to flow onto the bearing disk surface at a controlled rate of about 500mL/min (16.9oz/min). Lubrication to the valve plate - cylinder block interface is provided by hydrodynamic lubrication, so a new pin design was required to produce this effect. Pins for the pin on disk wear testing were electrical discharge machined from a copper-infiltrated, PM steel axial piston pump cylinder block. The design of the pins (Figure 13) was selected to provide an area of contact, promoting the formation of a lubricating film of hydraulic fluid.

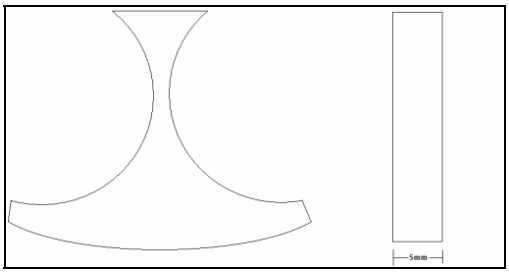

Figure 13. Drawing of pin for pin on disk.

The pins were loaded with 1745g (3.84 lbs) of weight, resulting in a contact area of 12.88 mm^2 (0.02 in^2) and an average contact stress between the pin and disk of 1.32MPa (191 psi). The maximum contact stress was calculated to be 1.69MPa (245 psi). Both of these values fell within the range of stresses (1.290 to 2.54 MPa, 187-368 psi) present on the bearing surface in the axial piston hydraulic pumps used for this study [6].

The disks for the wear tests were comprised of the production, experimental and newly developed valve plate materials. Wear testing samples of the Cu-10Sn-10Pb and Cu-10Sn-3Bi bearing bronzes were attained by utilizing production-ready valve plates. Wear specimens of the Cu-10Sn/Sn-1.37Mn and Cu-10Sn/Sn materials were created in a manner similar to the smaller samples used for initial alloy development. Tin-bronze powder was pressed at 350MPa (50.8 ksi) and sintered at 650°C (1202°F) for 2 hours to form 10mm (0.4 in) thick disks. The disks were then infiltrated, and the disk was polished to a surface roughness equal to that of the production valve plates.

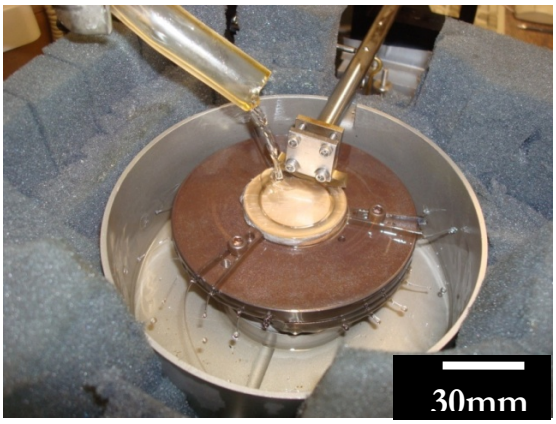

Figure 14. A lubricated wear test in progress.

Figure 14 depicts the wear test in process. All three samples exhibited a slight break-in period over the first few meters of sliding. Leaded bronze had the longest of the break-in periods, followed by bismuth and tin bronze. The average coefficient of friction (COF) for each of the materials was similar. The Cu-10Sn-10Pb valve plate material had an average COF of 0.18, the Cu-10Sn-3bi averaged 0.19, and each of the tin-infiltrated samples had a coefficient of friction of 0.17. Each of these is within the error of the friction measurement.

The HommelWerke LV-50 profilometer profiled across the diameter of the sample in three traces approximately 120 degrees apart. The traces were then evaluated using the HommelWerke TurboRoughness software. Each trace was then used to determine the inner and outer radius of the wear track. The software also calculated the area for each of the six wear track cross sections that resulted. The

wear volume loss was calculated using each of those six areas and averaged for the final result. The results of the calculations of volume loss due to wear are shown in Table II. The new tin-infiltrated bronze (Sn/Cu-10Sn) had the least volume loss of the three materials under lubricated sliding and resulted in less pin volume loss than the leaded bronze. The high volume loss in the leaded bronze sample was likely due to deformation in the soft material. The asperities on the surface of the leaded bronze are much deeper than those of the other two materials, allowing the surface to deform more under load.

Table II. Lubricated Sliding Volume Loss Due to Wear

Sample material	Disk volume loss (mm^3)	Pin volume loss (mm^3)
Cu-10Sn-10Pb	0.612	0.201
Cu-10Sn-3Bi	0.446	0.063
Sn/Cu-10Sn	0.353	0.104

Each material performed similarly in pin on disk testing under lubricated conditions. The primary form of wear for the Cu-10Sn-10Pb, Cu-10Sn-3Bi and Sn/Cu-10Sn bearing alloys was a mixture of plowing and abrasive wear caused by the asperities on the opposing surface. The primary difference in the tin-infiltrated bronze (Sn/Cu-10Sn and Sn-1.37Mn/Cu-10Sn) samples was the dominant presence of the soft phase. In the higher magnification image to the right in Figure 15, it can be noted that a small portion of the Cu_6Sn_5 that once rimmed the pore was pulled out. The Cu_6Sn_5 appeared to have been on the surface in the form of sub-micron particles. Tin also appears to have been drawn onto the surface. The presence of either the Cu_6Sn_5 particles or the free tin could not be confirmed with EDS because of their scale.

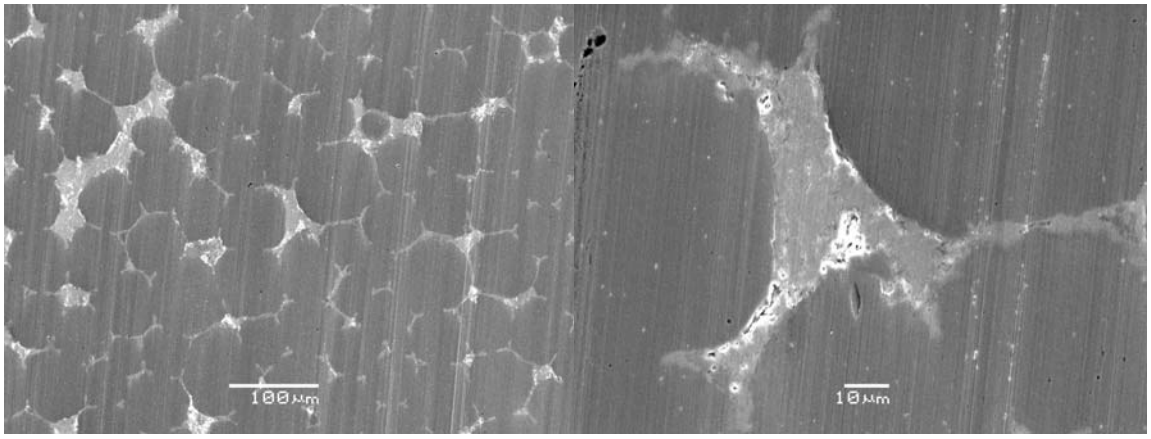

Figure 15. Appearance of the tin-infiltrated bronze wear track in the SEM.

The morphology of the soft phase in the wear track of the tin-infused bronze wear sample is quite different from the leaded and bismuth bronzes, as shown in Figure 16.

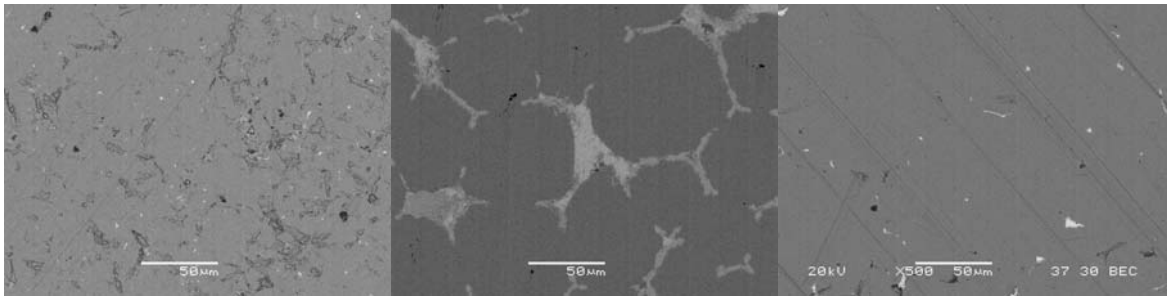

(a) (b) (c)

Figure 16. Soft phases in a) Cu-10Sn-10Pb b)Sn/Cu-10Sn and c) Cu-10Sn-3Bi tracks.

Although the distribution of soft phases appears different in the wear track, comparison of the visible soft phase in the Sn/Cu-10Sn wear sample shows that it was nearly identical to that produced in the original infiltration samples (Figure 17). Those original production samples were compared to the leaded and bismuth bronze valve plate microstructures in Figure 11 and were very similar. The deformation of the bronze material in the leaded and bismuth bronzes likely masks the soft phase. In the tin-infiltrated bronze, the fine, hard intermetallic particles produced by the breakup of the rim of intermetallics in each pocket may act as a mild abrasive. These particles are not large enough to affect the wear rate, but they scour the surface of the wear track keeping it free of adhesive bronze and exposing the soft phase.

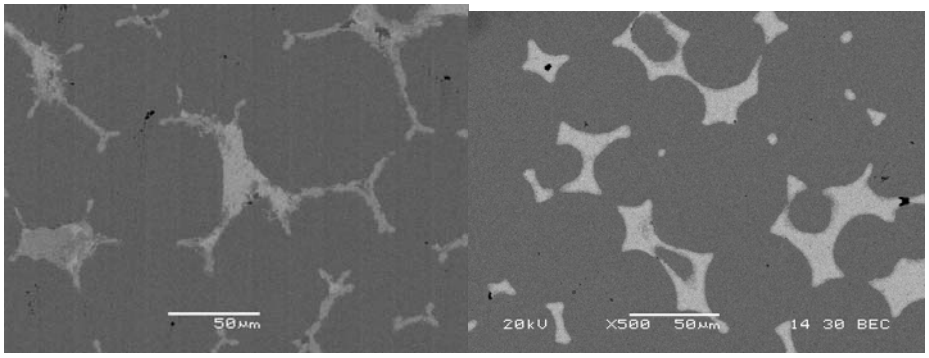

(a) (b)

Figure 17. Soft phase distribution on the a) wear track and b) polished of Sn/Cu-10Sn.

DISCUSSION

A novel lead-free alternative to leaded bronze bearing surfaces was developed that utilizes free pockets of tin or tin alloy in a bronze matrix, building from the idea that lead and tin have long been used interchangeably as soft bearings. Given proper processing parameters, liquid infiltration of a presintered porous bronze compact was shown to be a viable method of producing the bearing material, overcoming the issue of the solubility of tin in bronze.

The infiltration method does not, however, prevent the diffusion of tin into the copper-bronze matrix. Solidification of the soft tin alloy created copper-tin intermetallics where it contacted the bronze in the infiltrated microstructure. In small volume fractions, these intermetallics have been shown to be beneficial for several properties. However, having a highly networked boundary of a hard, brittle intermetallic phase could prove to be a detriment to impact strength, toughness and wear properties.

The extent of the intermetallic compound layer formation, particularly Cu3Sn, at the interface with the bronze matrix should be controlled to retain as much of the soft phase as possible. Initial control was achieved by minimizing the amount of heat exposure (temperature and time) required for infiltration of the porous Cu-10Sn bronze. Mitigation of the influence of intermetallic growth after thermal aging, particularly of Cu_3Sn, was also attempted by the minor alloy addition of manganese to the tin. From tests that were performed at a temperature (130˚C, 266°F) likely to be experienced during operation of the valve plate, the addition of manganese did slow the growth of Cu_3Sn compared to unalloyed tin, but it had no effect on the overall intermetallic layer thickness.

To promote the success of the melt infiltration processing approach, samples produced throughout this study were made from bronze compacts pressed at 350MPa (50.8 ksi) and sintered at 650°C (1202°F) for 2 hours. These compact production parameters were at the minimum green strength limits for handling and were designed to produce only modest sintered strength from the early stages of sintered neck growth. Even so, the porous bronze structures developed for this study displayed mechanical properties that approach that of the leaded bronze and bismuth bronze alloys previously developed.

In wear tests designed to simulate conditions in axial piston hydraulic pumps, the engineered tin-infiltrated bronze bearing material showed the same general wear mechanism as the leaded bronze and bismuth bronze. However, the Sn/Cu-10Sn alloy had the lowest volume loss of the three bearing alloys, even in 350MPa/650˚C/2hr (50.8ksi/1202°F/2hr) low green strength samples. It also possessed the lowest coefficient of friction, although the figure was not statistically different from the leaded and bismuth bronzes.

These results show that the basis for a new lead-free bearing alloy was successfully developed, and indeed warranted a provisional patent application [11]. However, there is a considerable amount of opportunity to fine tune the engineered structure of the composite material and the processing techniques used to produce it. Simple variations in processing parameters of both the bronze compacts and the infiltration of tin-based alloys have the capacity to change the composite microstructure for various applications. Optimization of the compaction and sintering parameters to balance the level of porosity in the bronze while retaining the proper strength will allow the material to be tailored to specific tribological systems. In addition, the control of the intermetallic growth, borrowing from the lead-free solder arena, will increase the lifetime of the material for an effective, lead-free bronze bearing material.

1. W.A. Glaeser, *Materials for Tribology*, 1992, Elsevier, New York.

2. B. Lunn, “Wear Resistance of Tin Bronzes and Related Alloys”, Wear, 1965, vol. 8, no. 5, pp. 401-406.

3. European Union. “Commission Decision of 13 October 2005 amending for the purposes of adapting to the technical progress the Annex to Directive 2002/95/EC of the European Parliament and of the Council on the restriction of the use of certain hazardous substances in electrical and electronic equipment”, http://www.reachcompliance.eu/english/legislation/docs/launchers/launch-2005-717-EC.html.

4. D.M. Saxton, “Lead-Free Replacements for SAE 792 in Bushing Applications”, 2006, Federal Mogul Corporation, SAE International.

5. G.A. Vetterick, “Lead-free, bronze-based surface layers for wear resistance in axial piston hydraulic pumps”, 2010, M.S. Thesis, Iowa State University, Ames, Iowa.

6. D. Wills, S. Hall, M. Betz, Sauer Danfoss Corporation, Ames, Iowa, private communication.

7. B. Bhushan, *Modern Tribology Handbook,* Volume 1, Mechanics and Materials Science Series, CRC Press, Florida.

8. D.R. Frear, J.W. Jang, J.K. Lin, and C. Zhang. “Pb-Free Solders for Flip-Chip Interconnects”, JOM, 2001, vol. 53, no. 6, pp. 28-32.

9. F. Thümmler, and R Oberacker, *Introduction to Powder Metallurgy*, 1993, The University Press, Cambridge.

10. A.V. Nenakhov, and A.G. Kostornov. “Tribological Characteristics Of Materials Based On Bronze For Small Friction Assemblies”, 2003, vol. 42, no. 7-8.

11. I.E. Anderson, G.A. Vetterick, M. Besser, “Lead-free Bronze-based Bearing Material and Method of Making”, U.S. Provisional Patent No. 61/337,672, March 17, 2010.